

Microstructure and Thermal Properties of Selective Laser Melted AlSi10Mg Alloy

Pin Yang*, Mark A. Rodriguez, Daniel K. Stefan, Amy Allen, Donald Bradley, Lisa Deibler, and Bradley H. Jared,
Sandia National Laboratories, Albuquerque, NM

Abstract

Powder bed laser additive manufacturing (AM) technique is widely used to fabricate complicated three-dimensional structures. Parts made by this fast melting and rapid solidification process are usually not at their equilibrium state. Additionally, the directed energy deposition by the laser beam can produce crystallographic texture and anisotropic properties. The driving forces imparted by this non-equilibrium state, such as stored elastic strain energy and chemical potential, can be invoked by an annealing process, which results in metallurgical changes such as stress-relief, recrystallization, and diffusion. This work investigates and compares the thermal properties of AM fabricated aluminum alloy with and without thermal annealing. Special focus is placed on the non-equilibrium state induced lattice imperfections and microstructure evolution on the thermal properties during the annealing process. These changes will be compared to the calculated phonon and electron mean-free-paths to identify the key issues governing the changes in thermal properties during the annealing process. These implications are important to ensure the thermal performance of AM fabricated AlSi10Mg parts and other solution treatable alloys for practical applications.

AlSi10Mg Alloy:

- Low density, high strength and hardness, good thermal properties
- Low melting point – close to eutectic temperature (hypoeutectic)

Non-equilibrium process (AM) induced issues related to thermal properties:

- Three levels of microstructure, i.e., melt zone, grain size, and divorced cellular structure
 - Lattice imperfections, i.e., dislocation, oversaturated lattice, porosity, residual stress
- These factors enhance anharmonicities of lattice vibration and scattering for the Umklapp processes.

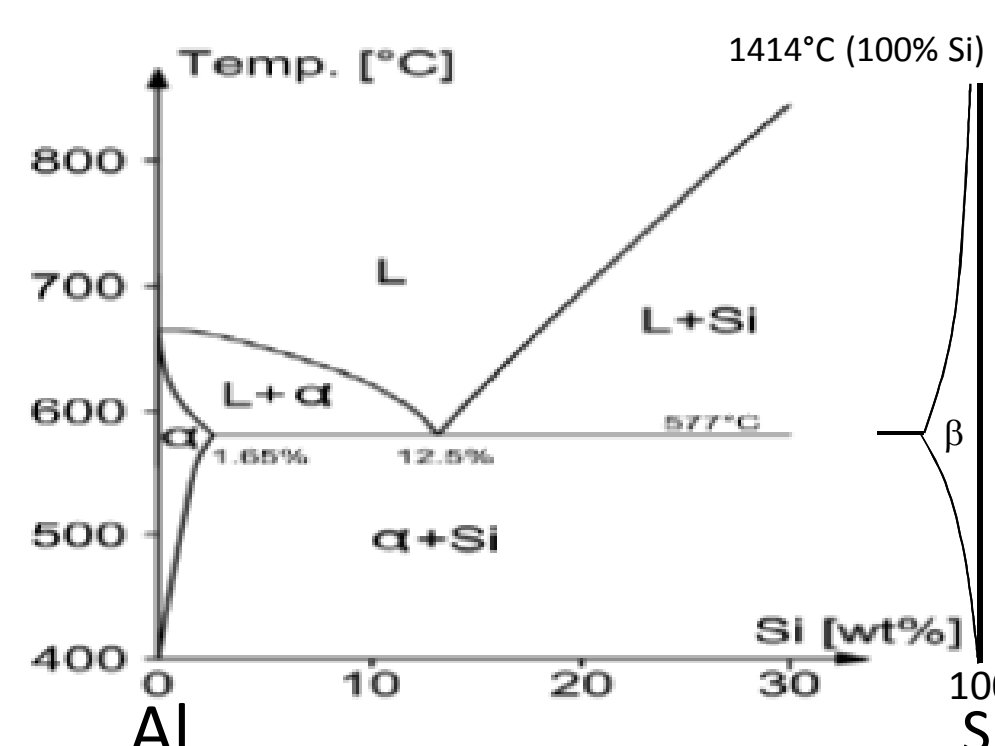


Fig 1 Partial phase diagram for AlSi10Mg and existing phases (not including fine, strengthening precipitates such as β'' and β').

Texture and Residual Stress

- XY samples have a typical (200) out of plane orientation, while the Z samples show a (200) rolling texture.

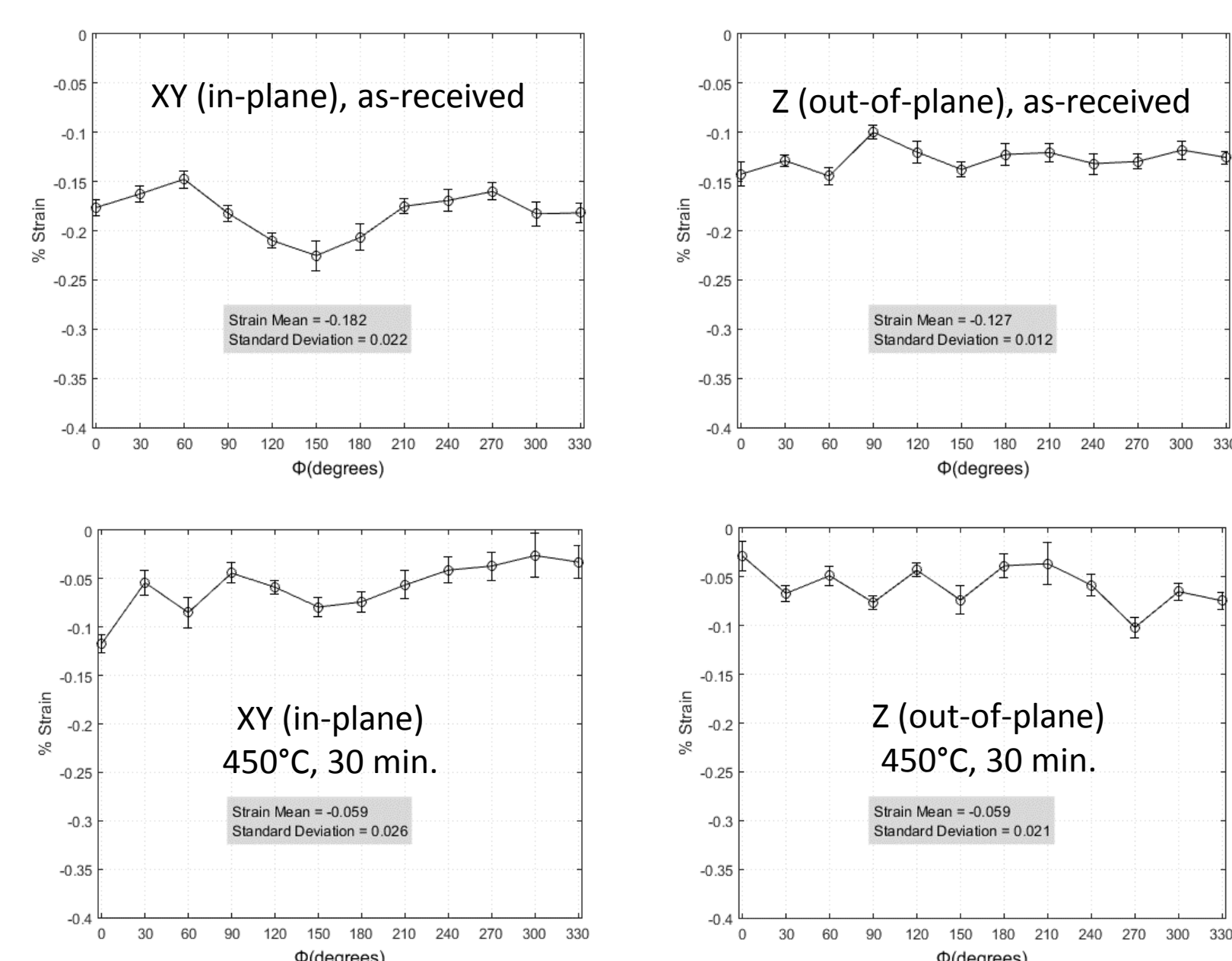
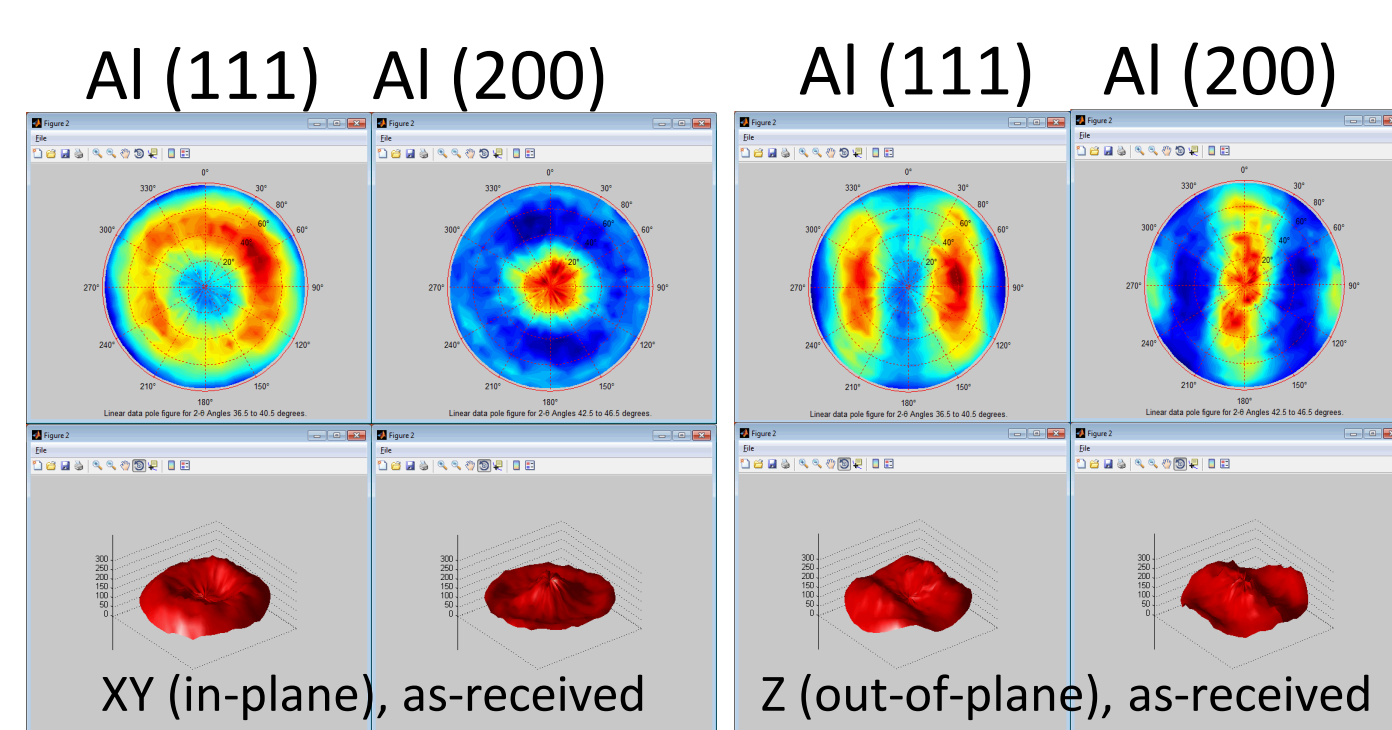


Fig. 5 Tilt-whirl 2D pole figure results and Phi rotation values vs. % strain plots.

- The compressive in-plane strains presented in the as-built samples are initially significant, with values in the -0.18% for the XY samples and -0.13% for the Z samples. Heat treatment significantly decreases residual strain values down to about -0.06% for both the XY and X samples.

Summary

- The thermal properties of the as-built and the stress-relieved parts fabricated by the SLM process are significantly different. The stress-relieved parts are isotropic, while the as-received samples exhibit an anisotropic behavior with significant residual stress and texture.
- Thermal treatments above the Debye temperature of aluminum heal lattice defects, promote phase segregation/precipitation, reduce the residual stresses, and coarsen the microstructure.
- By aggregating excess Si atoms into large precipitates, removing lattice defects and coarsening the microstructure, thereby increasing the mean-free path between scattering centers, the thermal diffusivity and thermal conductivity can be drastically improved. In addition, the collapsing of the cellular structure above 282°C also contributes to the improvement of heat transfer.
- These implications are important to ensure the thermal performance of AM fabricated solution treatable alloys for practical applications.

Microstructure Evolution as a Function of Temperature

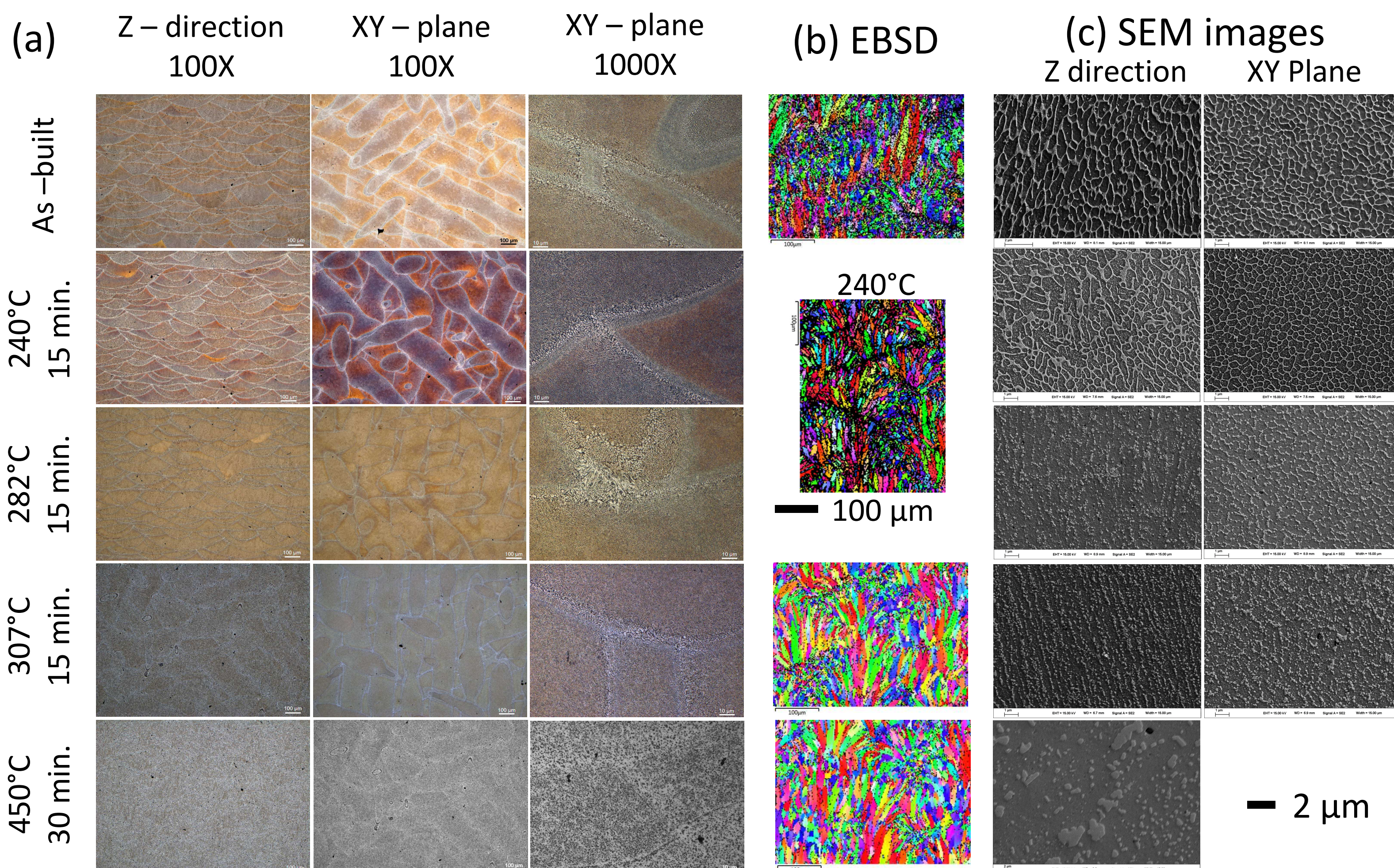


Fig. 2 Microstructure evolution as a function of temperature (a) optical images of melt and heat affected zone (HAZ) (hundreds of microns), (2) EBSD images of grain structure parallel to build direction showing porosity aggregated at HAZ (tens of microns), and (3) SEM images for the microstructure evolution of the divorced cellular structure.

Heat Capacity (C_p), Thermal Diffusivity (α) and thermal conductivity (λ)

- The DSC curves of a stress-relieved sample all lie on top of each other, while the as-built samples shows a double-exothermic peak on the first heating.
- It is believed that first large exothermic peak below 300°C comes from the release of stored elastic strain energy and the formation of Mg_2Si precipitates[†] in the super-saturated AlSi10Mg solid solution. [†]I. Dutta, and S.M Allen, J. Mater. Sci. Lett. (1991).
- In-situ X-ray analysis indicates that excess silicon in the quenched alloy starts to segregate in an accelerated rate from the nanocrystalline divorced eutectic structure at 275°C as well as the formation of rod-shape β' precipitates* above 300°C contributing to the second exothermic peak between 270°C and 340°C . * M. I. Daoudi, A. Triki, and A. Redjaimia, J Therm. Anal. Caborim (2011).
- Data suggest that there is a significant electron and phonon scattering below 150°C

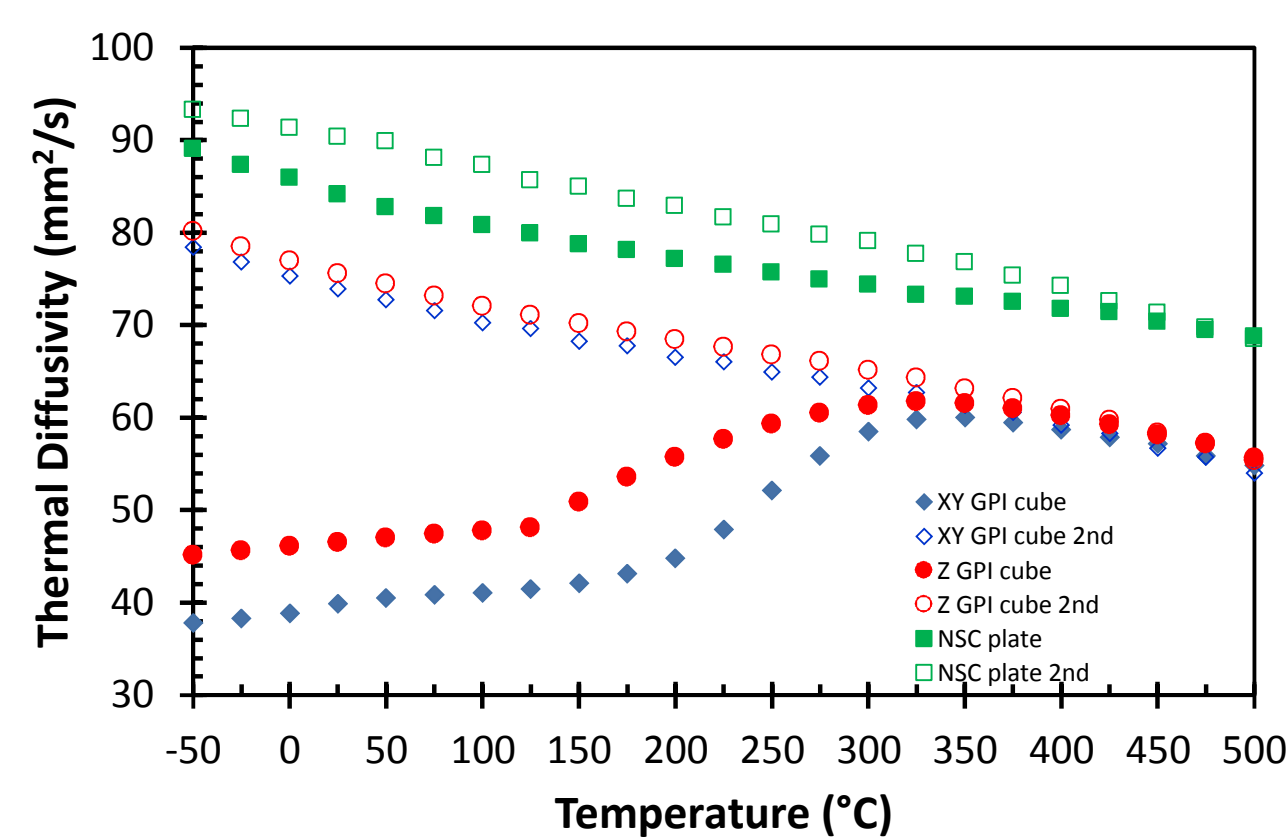
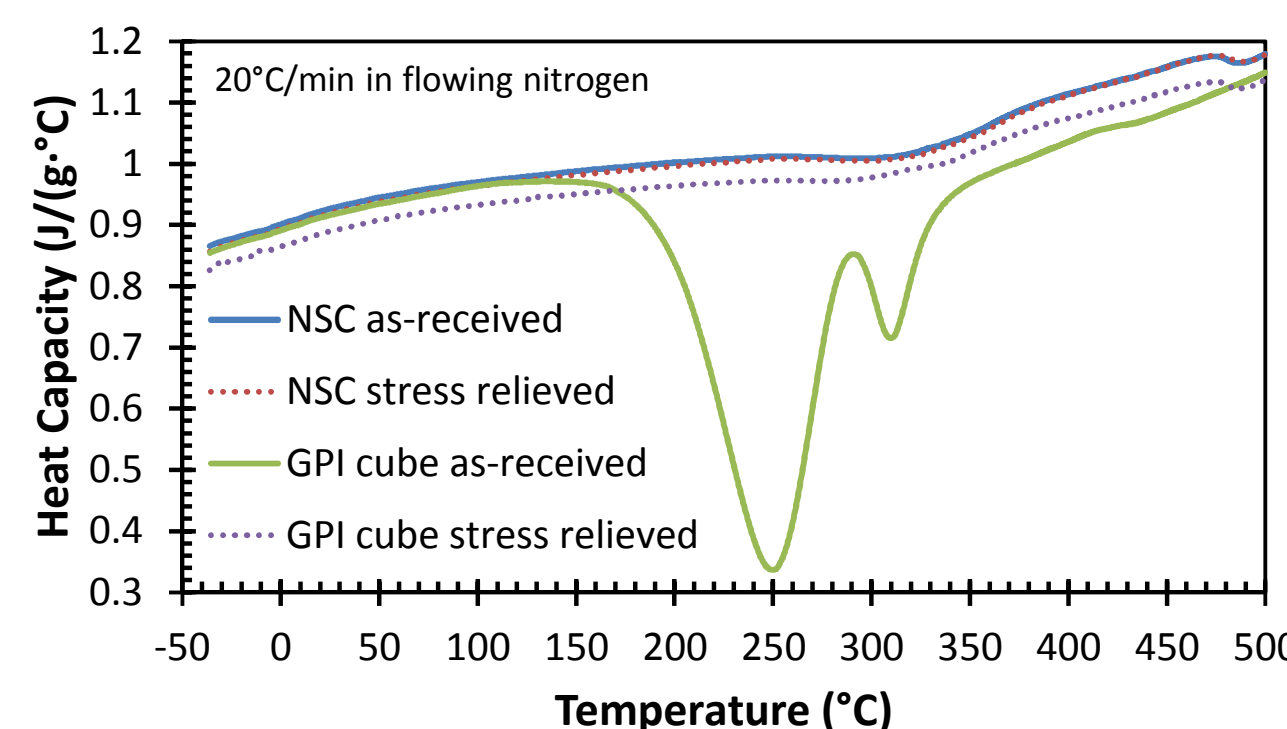


Fig. 7 Thermal diffusivity of as-built and stress relieved samples as a function of temperature.

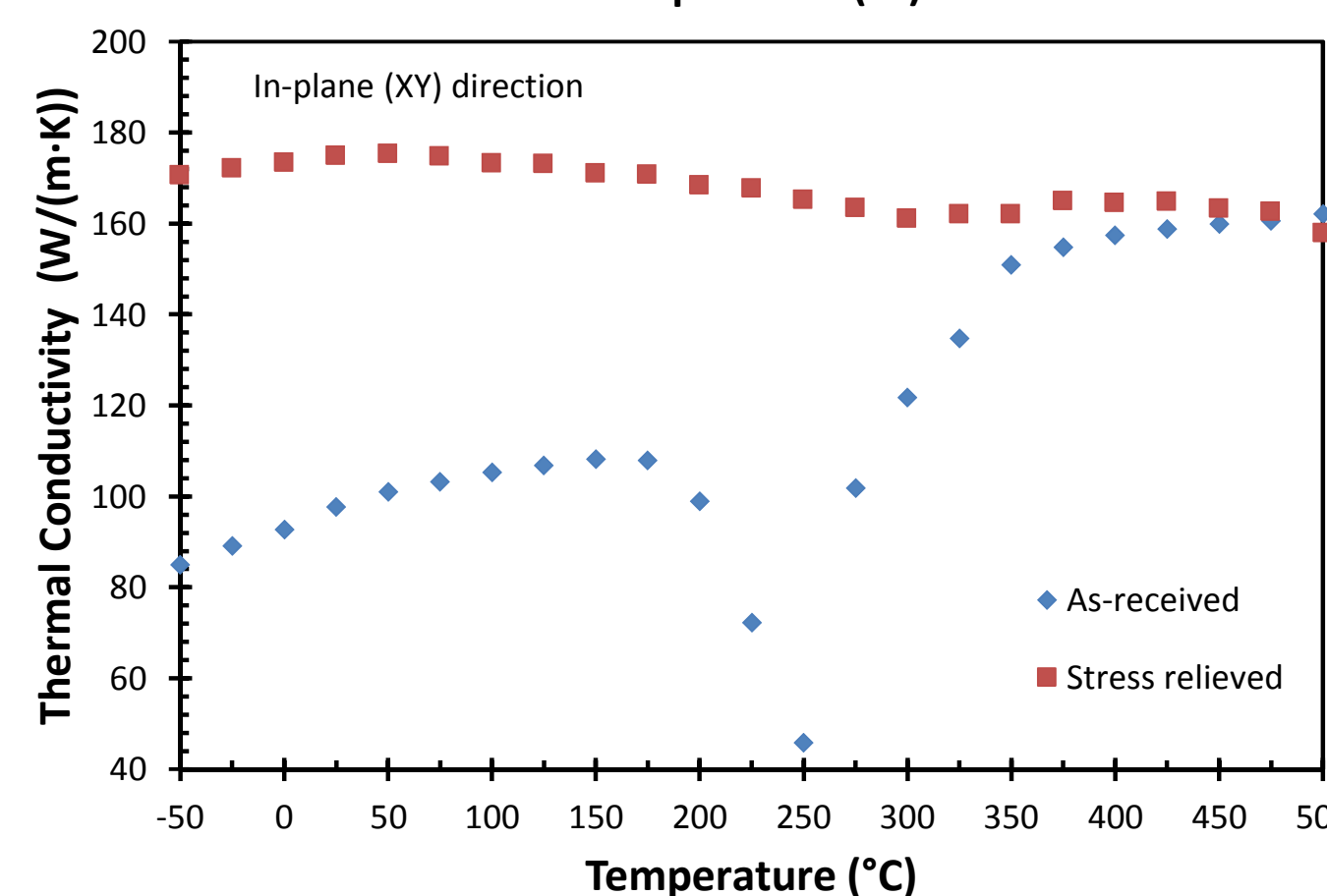
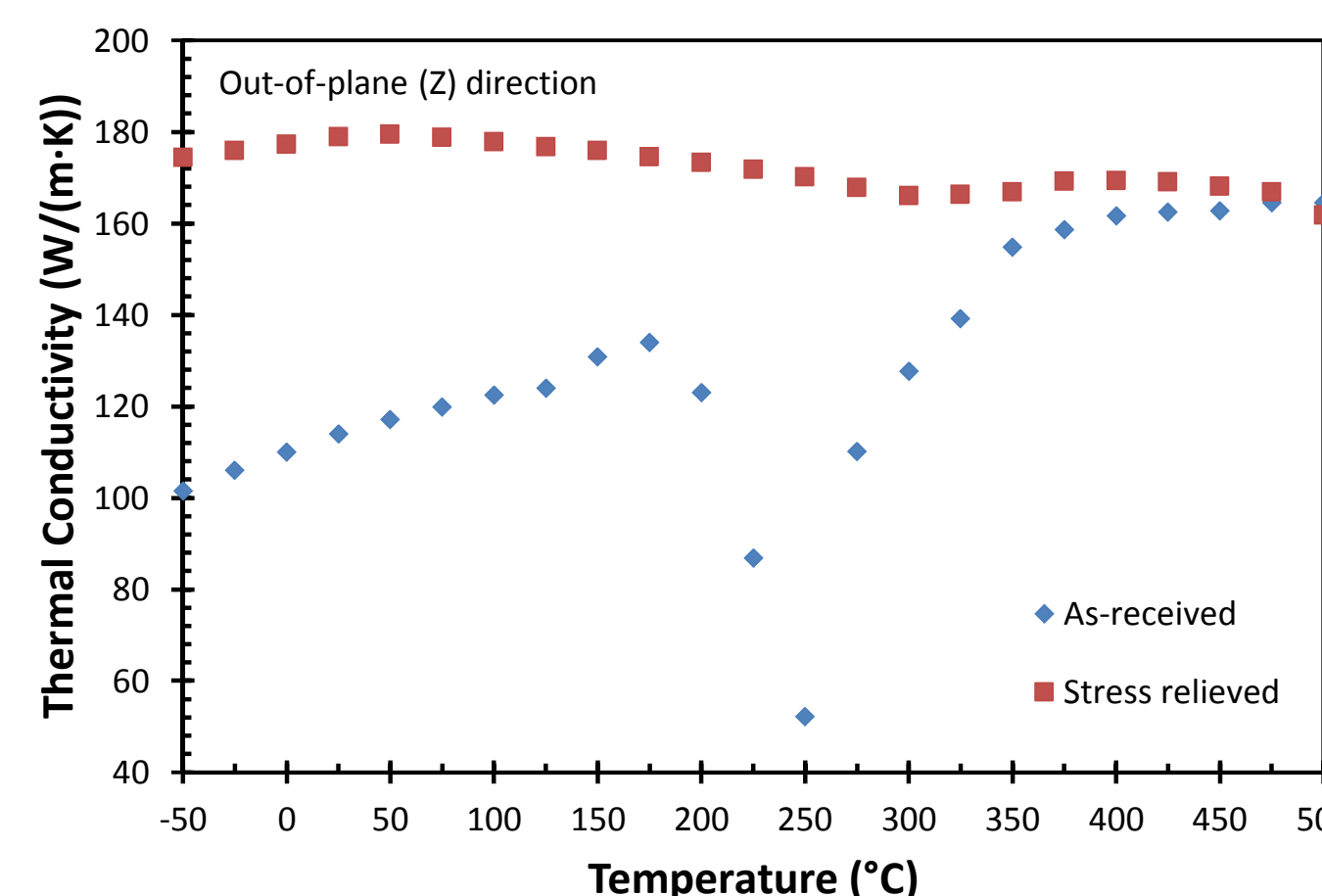
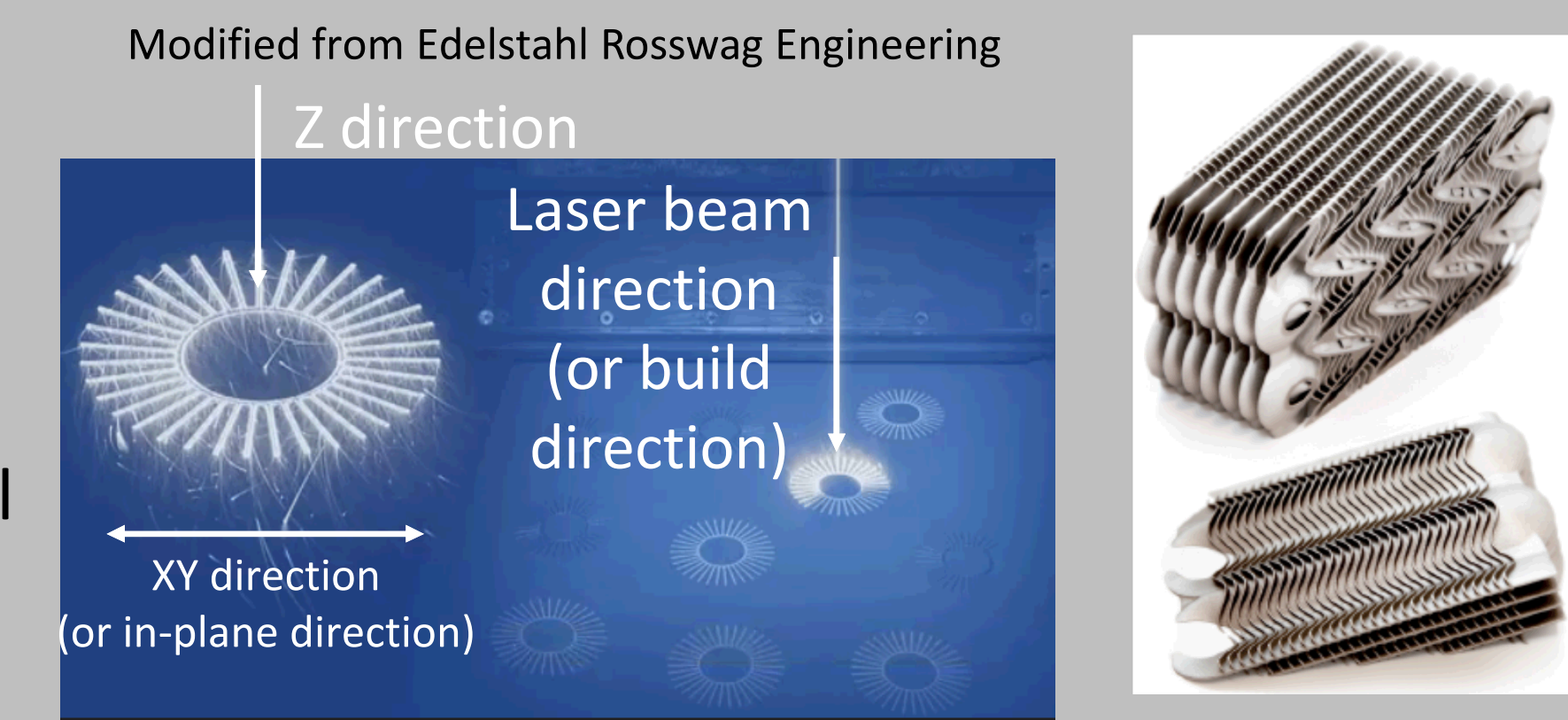


Fig. 8 Thermal conductivity before and after heat treatment.



www.3trpd.co.uk

- No significant microstructure change, except excess Si starts to precipitate out with in the cellular structure below 240°C ,
- Above 282°C , the cellular structure collapses, grain growth is observed, the shape of the melt zone defined by the heat affected zone (HAZ) becomes less obvious.
- Heating above 308°C ., the HAZ starts to disappear and excess Si atoms begin to aggregate and develop a particle free zone*; therefore, the microhardness decreases significantly.

*L. Pedersen and L. Arnberg, Metall. Mater. Trans. A (2001).

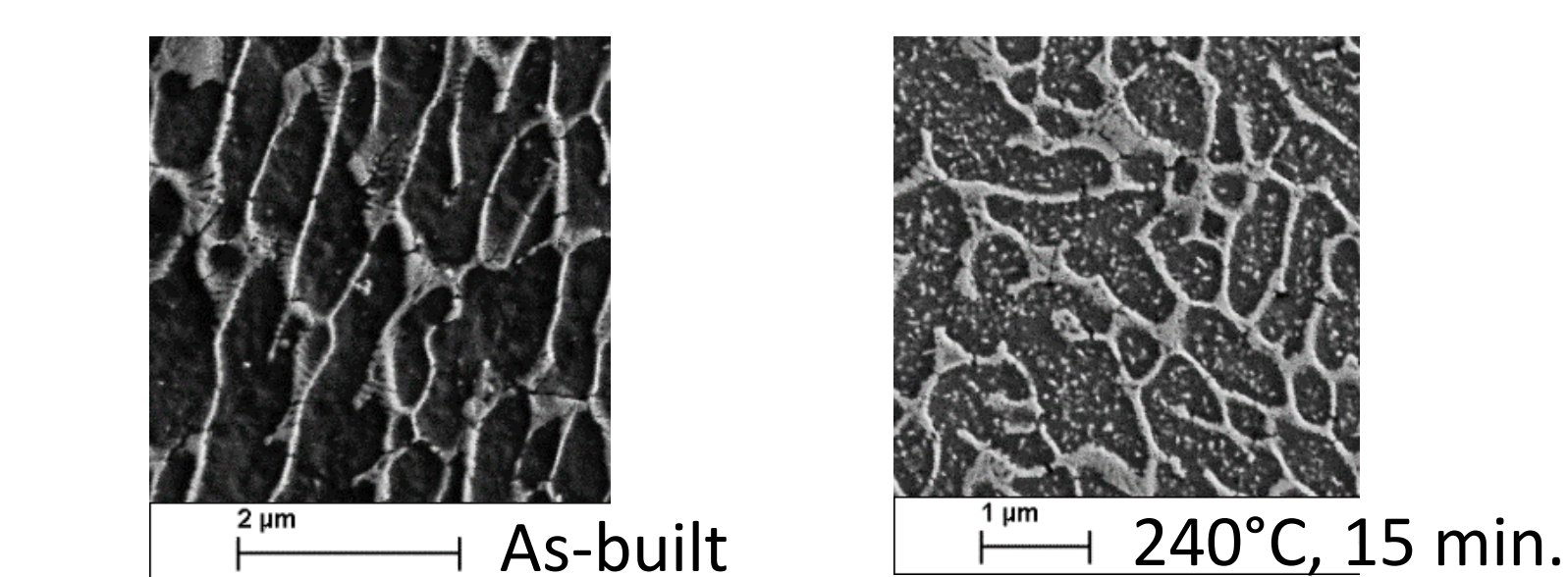
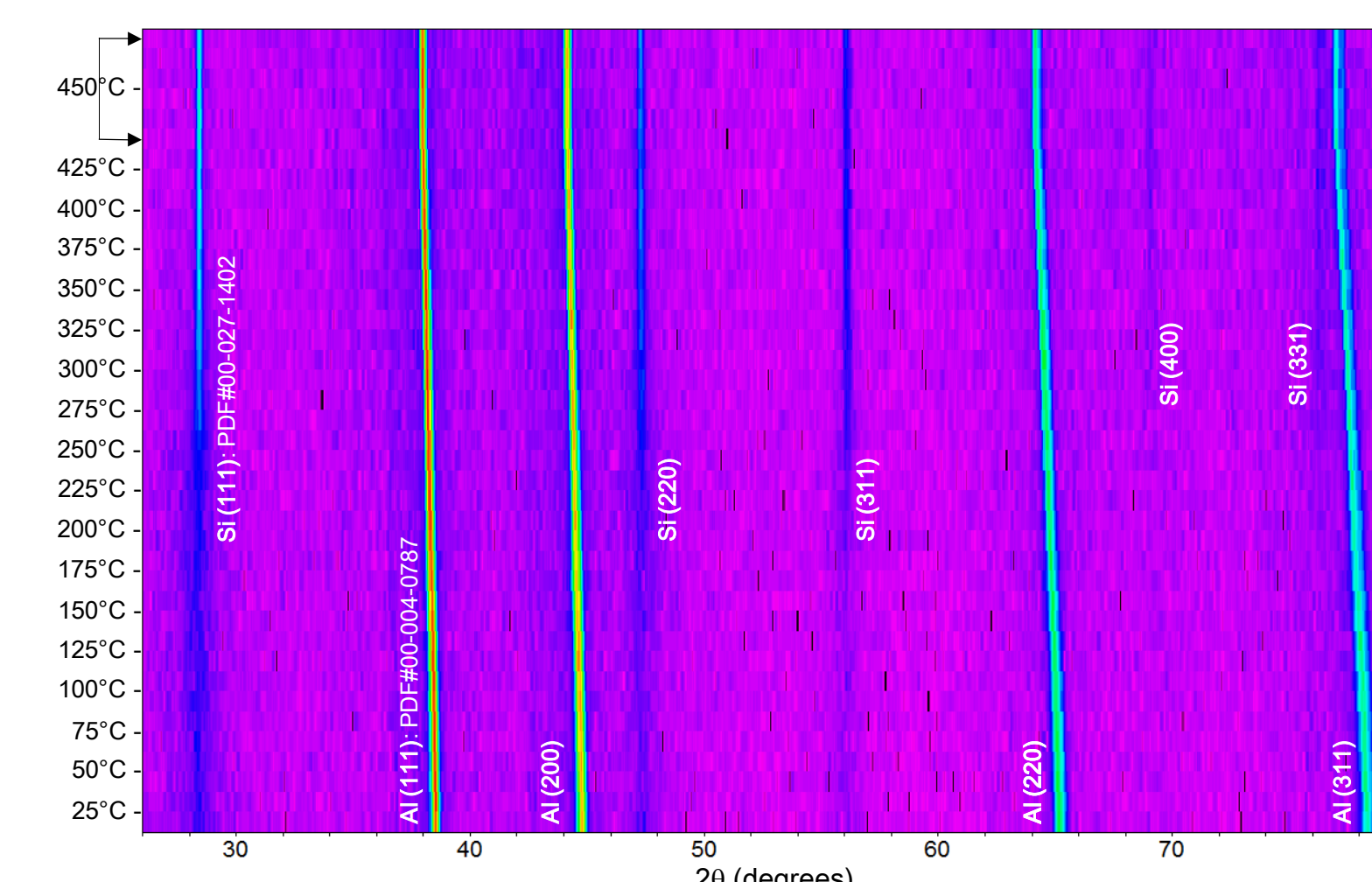


Fig. 3 The dissolution of Si as a function of temperature.

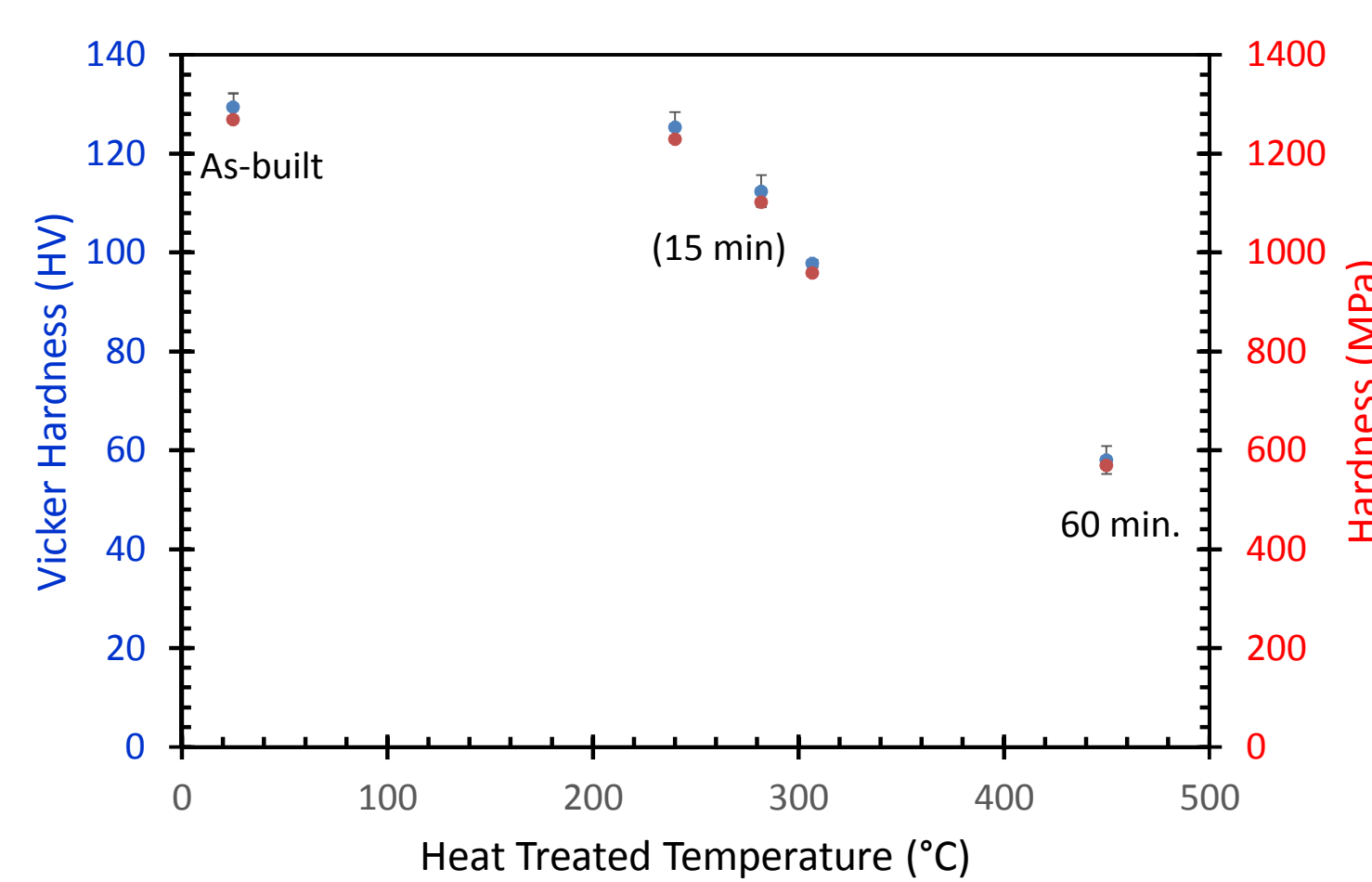


Fig. 4 Change of microhardness by thermal treatment.

Calculated Thermal Properties

Table 1: Room Temperature Material Properties for Aluminum and Al Si10Mg Alloy from Literature* and Calculation.

	Electronic Contribution to Thermal Properties		Reference
	Free electronic density – (e/m^3)	1.809 $\times 10^{29}$	
Al	Fermi Level (E_F) at 0 K – (eV)	11.66	
	Electron velocity at Fermi Level (v_F) – (m/s)	2024917	
	Time between collision (τ) – (s)	7.16×10^{-15}	
	Electron mean-free-path (l_e) – (Å)	145.1	
	Electrical conductivity* (σ_e) – ($\text{Ohm}^{-1} \text{cm}^{-1}$)	365×10^3	REF
	Calculated thermal conductivity (σ_e) – (W/m·K)	267.7	
	Thermal conductivity* (α_e) – (W/m·K)	237	NIST
	Phonon Contribution to Thermal Properties		Reference
	Atomic density (atoms/ m^3)	6.029×10^{28}	
Al	Mean acoustic velocity* (v) – (m/s)	3666	Kittle
	Debye Temperature* – (K)	428	Kittle
	Averaged phonon mean-free path ($3\lambda/C_v$) – (Å)	80.0	
AlSi10Mg	Longitudinal sound velocity (m/s)	6453	
	Shear sound velocity (m/s)	3119	
	Average acoustic velocity (v) (m/s)	3507	
	Debye temperature (K)	409	
	Thermal diffusivity (α_e) – (m^2/s)	4.648×10^{-6}	
	Averaged phonon-mean-free Path from ($3\lambda/C_v$) – (Å)	39.8	

- Both electron and phonon scatterings are below 150°A .
- Heat transfer is controlled and dominated by the lattice imperfection and oversaturated lattice blow 150°C .